PHOTODEGRADATION OF BENZENE, TOLUENE, *p*-XYLENE IN AQUEOUS PHASE USING ZnO, TiO$_2$, SnO$_2$, WO$_3$ and Fe$_2$O$_3$ PHOTOCATALYSTS PREPARED VIA SOL-GEL METHOD

Zul Adlan Mohd Hir[1*], Rusmidah Ali[2]

[1]Faculty of Applied Sciences, Universiti Teknologi MARA Pahang, 26400 Bandar Tun Abdul Razak Jengka, Pahang

[2]Faculty of Science, Universiti Teknologi Malaysia, 81310 Johor Bahru, Johor

[*]Corresponding author: zuladlan@uitm.edu.my

Abstract

Aromatic volatile organic compounds (VOCs) such as benzene, toluene and *p*-xylene (BTX) have been long considered as carcinogenic and toxic to humans as well as environmentally harmful. The continuous exposure to these compounds could cause neurasthenia and even leukemia. Therefore, necessary actions should be taken to combat the presence of these compounds in water. In this work, the photodegradation of BTX mixture was carried out using five different types of semiconductor oxides prepared via sol-gel method, namely ZnO, TiO$_2$, SnO$_2$, WO$_3$ and Fe$_2$O$_3$ with UV-light centered at 365 nm. The band gap energy for all prepared photocatalysts was estimated from Kubelka-Munk function. The suitability of the band gap of ZnO (3.20 eV) and TiO$_2$ (3.00 eV) envisages the best degradation performances at 0.10 g loading for both photocatalysts, by degrading ~42% BTX mixture in original condition. Such photoactivity is mainly ascribed to photons energy absorption and efficient separation of photoinduced electron–hole pairs derived from the photocatalysts. This further promotes the formation of reactive radicals' species which responsible for the bond-breaking of the VOCs.

Keyword: Photocatalysis, semiconductor oxide, sol-gel, volatile organic compounds

Introduction

The expanding organic environmental pollution especially by volatile organic compounds (VOCs) has become a worldwide concern which not only affects human health but also impedes the economy and society developments. VOCs exist extensively in both outdoor and indoor environments which have direct and long exposure to human health. The main sources of VOCs are leaking of fuels from old underground storage tanks, motor vehicle exhaust, detergents, paints, wall boards, varnishes, petroleum products, pharmaceuticals, and etc. (Binas et al., 2019; Bustillo-Lecompte et al., 2018) The serious implications to human health such as nausea, headache, tiredness, increased heart rate, vomiting and convulsions is a grave issue apart from metabolic transformation of these compounds by specific enzymes resulting toxicity in human body, damaging the blood cells and could possibly lead to leukemia (Binas et al., 2019; Leusch & Bartkow, 2010). According to World Health Organization (WHO), the maximum allowable concentrations of benzene, toluene and xylene in water are 0.01, 0.7 and 0.5 mg/L, respectively (Ferrari-Lima et al., 2015; WHO, 2004)

Although there are variety of available water treatment approaches, photodegradation by semiconductor oxides has been chosen due to its capability to mineralize VOCs in water (Ahmed et al., 2018). Semiconductor metal oxides are regarded as versatile materials that can be used for several applications including electronic, energy harvesting, medical and sensor

material as well as environmental pollution control. By understanding the surface chemistry of metal oxides, the physicochemical properties can be exploited as photocatalyst for water remediation process. In this case, when the metal oxides are exposed to light irradiation, there will be photoexcitation of electrons from the valence band (vb) to the conduction band (cb). The excitation of electrons would simultaneously generate positive holes (h^+) in the vb, and subsequently labeled as photoinduced electron-hole pairs. Over sequence of reactions between electrons and adsorbed O_2 (reduction) and between holes and adsorbed H_2O (oxidation), reactive radical species will be formed (Hir et al., 2017). It is suggested that hydroxyl radicals (•OH) and superoxide radical anions (•O_2^-) are the main reactive species responsible for the degradation of the pollutant in water. Therefore, the aim of the current study is to synthesize single photocatalysts of ZnO, TiO_2, SnO_2, WO_3 and Fe_2O_3 via sol-gel method and to evaluate their individual photocatalytic performance. Emphasis was placed on the suitability of the band gap energy (E_g) possesses by the photocatalysts towards BTX mixture degradation under UV-light irradiation centered at 365 nm.

Materials and Methods

Preparation of ZnO, TiO_2, SnO_2, WO_3 and Fe_2O_3 as single photocatalysts

i) Preparation of ZnO
Zinc acetate dihydrate, $Zn(CH_3CO_2)_2.2H_2O$ (0.5 g) was dissolved in 2-propanol (200 mL) with the temperature controlled at 50–60°C. Later, sodium hydroxide (10 mg) was added and stirred continuously before left in water bath at 25°C for 1 h.

ii) Preparation of TiO_2
Polyethylene glycol (PEG 2000) (6.0 g) was dissolved in ethanol (600 mL) and stirred continuously prior to the addition of diethanolamine (31.8 g), titanium isopropoxide (85.2 g) and deionized water (5.4 mL). The mixture was stirred continuously for another 3 h at 25°C to form a homogeneous solution.

iii) Preparation of SnO_2
Tin tetrachloride, $SnCl_4.5H_2O$ (17.5 g) was completely dissolved in a solution comprised of deionized water and ethanol (volume ratio is 1:1) and stirred continuously at 25°C until colourless solution formed.

iv) Preparation of WO_3
Tungstic acid, H_2WO_4 (5.4 g) was dissolved in 30% (w/w) hydrogen peroxide (100 mL) and stirred continuously until colourless solution formed. Then, polyethylene glycol (PEG 2000) was added and stirred for another 8 h at 25°C to form a homogeneous solution.

v) Preparation of Fe_2O_3
Iron trichloride hexahydrate, $FeCl_3.6H_2O$ (13.51 g) was dissolved in a solution comprised of deionized water and ethanol (volume ratio is 1:1) and stirred continuously at 25°C until colourless solution formed.

All resultant solutions were dried overnight in the oven at 80°C prior to calcination at 550°C for 5 h.

Preparation of benzene, toluene, *p*-xylene mixture solution
Benzene, toluene, *p*-xylene mixture solution (1000 ppm) was prepared by taking 285.23 µL of

benzene (density, ρ: 0.8765 g/mL), 288.38 µL of toluene (density, ρ: 0.8669 g/mL), and 289.35 µL of ρ-xylene (density, ρ: 0.8640 g/mL) in 250 mL volumetric flask. Then, distilled water was added to the mark. The solution was stirred continuously for 1 h at at 25°C as to give a slightly homogeneous solution. Later, the organic layers that formed were separated from the aqueous solution by using separating funnel. The aqueous solution (200 mL) was taken out and used as a working solution in this study.

Photocatalytic degradation system
The benzene, toluene, *p*-xylene (BTX) solution with concentration of 1000 ppm was put into a pyrex glass photoreactor and sealed with parafilm to avoid evaporation of the BTX compounds. Then, the working solution was stirred for 30 min to ensure uniform mixing. Later, the prepared photocatalysts (0.10 g) was added into the working solution and stirred in dark for another 30 min to attain adsorption-desorption equilibrium prior to illumination by UV-A lamp (6 W, λ = 365 nm) for 3 h. 10 mL of sample was drawn out at predetermined time intervals and the absorbance of the sample was analysed using UV-Vis Spectrophotometer (Model UV-2501PC Shimadzu) at λ_{max} = 260 nm. The percentage of photodegradation was calculated using the formula in Equation (1).

$$\% \text{ Degradation} = \frac{(C_o - C_t)}{C_o} \times 100\% \tag{1}$$

where C_o is the concentration of BTX before irradiation and C_t is the concentration of BTX at time 't'.

Results and Discussion

Crystal phase, band gap energy and photoactivity of ZnO, TiO$_2$, SnO$_2$, WO$_3$ and Fe$_2$O$_3$ photocatalysts
The crystal phase for all single photocatalysts of ZnO, SnO$_2$, WO$_3$, Fe$_2$O$_3$ and TiO$_2$ were acquired from X-ray diffraction analysis, and the data are illustrated in **Figure 1a–e**, respectively. Several characteristics of ZnO hexagonal phases were observed at 2θ values of 36.312° (101), 31.836° (100), 34.484° (002), 56.678° (110), 62.933° (103), 68.003° (112), 47.582° (102), and 69.155° (201). These peaks were assigned to their respective crystal plane exist in the bulk matrices of the catalyst according to JCPDS card no. 36-1451 (Hir et al., 2017). The major triplet peaks for WO$_3$ monoclinic phases were identified at 24.330° (200), 23.144° (002), 23.687° (020), 34.108° (202), 49.921° (400), 26.616° (120), 28.749° (112), 55.731° (142), 41.765° (222) and 62.247° (340) with moderately high intensity of characteristic peaks based on JCPDS card no. 83–0951 (Parthibavarman et al., 2018). In contrast, the high crystallinity of SnO$_2$ tetragonal phases were assigned to 26.552° (110), 33.851° (101), 51.754° (211), 37.938° (200) and 65.952° (301) with JCPDS card no. 77-0451 (Elci et al., 2018). While Fe$_2$O$_3$ rhombohedral phases were detected at 33.195° (104), 35.641° (110), 54.072° (116), 49.520° (024), 24.151° (012), 62.472° (214), 64.027° (300) and 40.863° (113) in accordance with JCPDS card no. 33-0664 (Fouad et al., 2019). It was also observed that the presence of TiO$_2$ rutile was more dominant as compared to TiO$_2$ anatase. The angles of reflections of TiO$_2$ rutile (JCPDS 00-021-1276) were occurred at 27.461° (110), 54.308° (211), 36.063° (101), 41.290° (111), 69.120° (301) and 56.582° (220) and low intensity of anatase peaks (JCPDS 00-021-1272) were observed at 25.294° (101), 47.936° (200) and 37.743° (004) (Hir, et al., 2017).
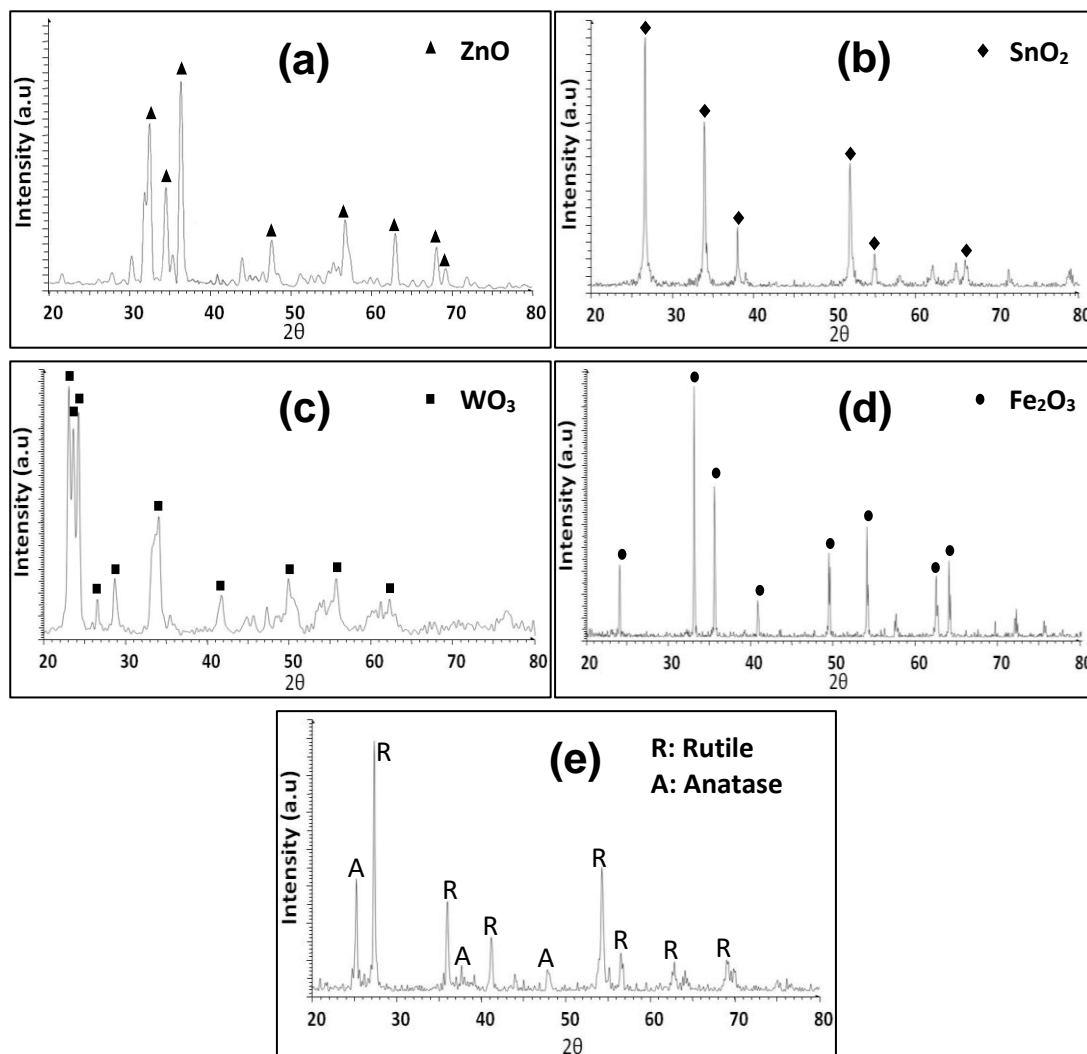
Figure 1 XRD diffractograms pattern of prepared single photocatalyst of a) ZnO; b) SnO$_2$; c) WO$_3$; d) Fe$_2$O$_3$; and e) TiO$_2$

The determination of the band gap energy (E$_g$) of the photocatalysts was carried out using UV-Vis Diffuse Reflectance Spectroscopy (UV-DRS). **Figure 2** shows that ZnO, TiO$_2$, SnO$_2$, WO$_3$ and Fe$_2$O$_3$ exhibited E$_g$ of 3.20, 3.00, 3.70, 2.70 and 1.50 eV, respectively. The energy provided by the UV lamp centered at 365 nm was estimated at around 3.40 eV. From the results obtained, ZnO, TiO$_2$, WO$_3$ and Fe$_2$O$_3$ were most likely favourable to absorb the photons energy provided by the UV-light which requires energy equal to or higher than its band gap energy. However, the ZnO displayed 0.17 eV less positive than the theoretical value of 3.37 eV while TiO$_2$ belonged to the rutile phase with 0.20 eV less positive than the E$_g$ of anatase phase (3.20 eV)(Fischer et al., 2017; Hir et al., 2017) Fe$_2$O$_3$ showed decreasing of its E$_g$ as compared to the theoretical value of 2.20 eV (Costa et al., 2020). The decreasing in the E$_g$ might be due to the increase in particle size, resulting from the higher calcination temperatures (>500°C) which led to the red shift of the absorption edges of the spectrum (Singh et al., 2018). On the other hand, SnO$_2$ demonstrates large E$_g$ of 3.70 eV slightly higher from the theoretical value (3.60 eV)(Karmaoui et al., 2018), indicating that the photon energy will be absorbed less. Consequently, the energy provided by the UV-light will be insufficient for the excitation of electrons and hence, lower photoactivity.
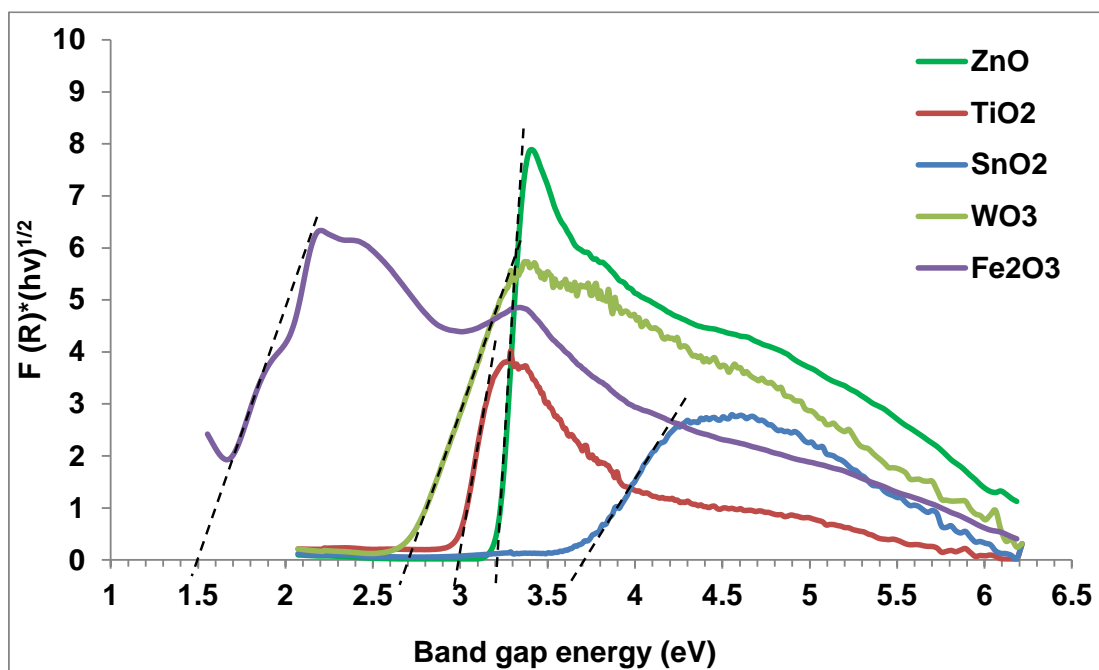
Figure 2 Plot of Kubelka-Munk function versus band gap energy for all prepared photocatalysts

Figure 3 shows the photocatalytic activities of ZnO, TiO$_2$, SnO$_2$, WO$_3$ and Fe$_2$O$_3$ photocatalysts in degrading BTX mixture under UV-light irradiation in a period of 210 min. In the absence of photocatalyst (photolysis), 15.37% of BTX was degraded. On the other hand, ZnO gave the highest degradation percentage of 42.97%, followed by TiO$_2$ which exhibited slightly lower degradation percentage (42.05%). However, when the BTX was treated with WO$_3$ and Fe$_2$O$_3$, the degradation percentage was decreased to 36.77% and 35.62%, respectively with SnO$_2$ gave the lowest degradation percentage of 31.04% due to large band gap. It was observed that the photocatalytic performance was influenced by the E$_g$ of the respective photocatalysts (Singh et al., 2018). Theoretically, when the catalyst particles are exposed under the light irradiation (photons) with energy equal to or higher than its band gap, it will result in the formation of photoinduced electrons (e$^-$) and positive holes (h$^+$) in the conduction and valence bands, respectively. These species will further react in a series of redox reaction between adsorbed oxygen and adsorbed water to produce •OH radicals. The formation of this powerful oxidizing agent (•OH) will have the aptitude to attack the BTX compounds present at the surface of photocatalyst (Syazwani et al., 2018). Consequently, it will mineralize the toxic compounds into harmless species such H$_2$O and CO$_2$ molecules.
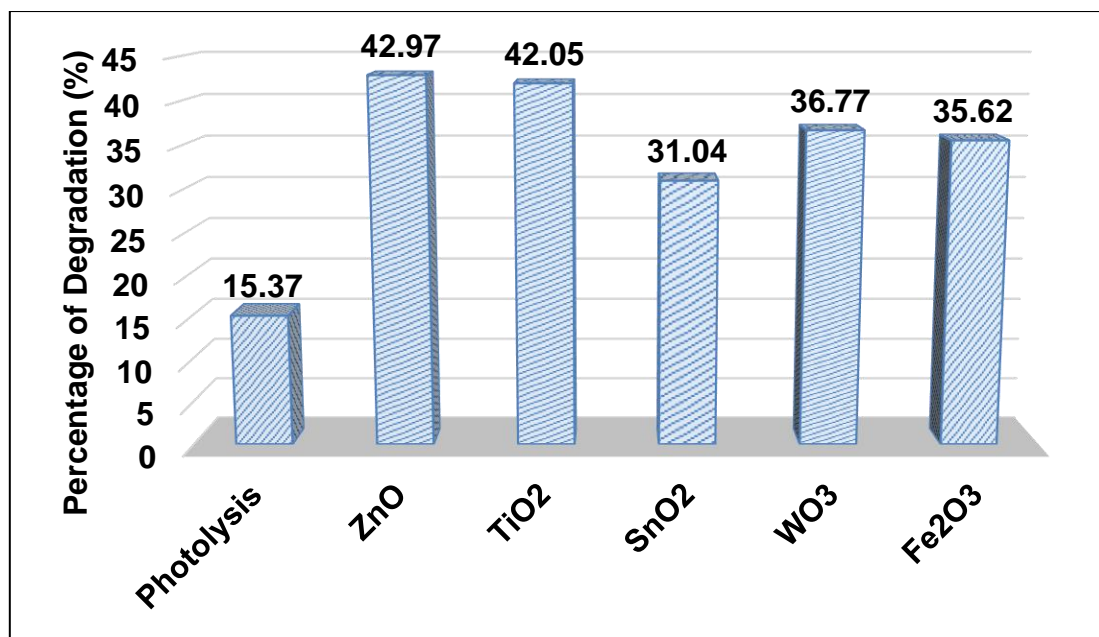
Figure 3 Photolysis and percentage degradation of BTX mixture

Conclusion

ZnO and TiO$_2$ were found to be the most effective photocatalyst where they exhibited higher photodegradation activity against BTX mixture under UV irradiation with degradation percentage of about ~42%. Band gap energy of the photocatalysts plays a crucial role in absorbing sufficient photons energy to initiate the formation of photoinduced electron-hole pairs so that the pollutant molecules can be effectively degraded at the surface of the photocatalysts in a timely manner.

Acknowledgement

Conflict of interests

The authors declare that there are no conflicts of interest associated with this publication, and there has been no significant financial support for this work that could have influenced its outcome.

References

Ahmed, G., Hanif, M., Khan, A. J., Zhao, L., Zhang, J., & Liu, Z. (2018). ZnO flowers and graphene oxide hybridization for efficient photocatalytic degradation of o-xylene in water. *Materials Chemistry and Physics*, *212*, 479–489. https://doi.org/10.1016/j.matchemphys.2018.03.067.

Binas, V., Stefanopoulos, V., Kiriakidis, G., & Papagiannakopoulos, P. (2019). Photocatalytic oxidation of gaseous benzene, toluene and xylene under UV and visible irradiation over Mn-doped TiO$_2$ nanoparticles. *Journal of Materiomics*, *5*(1), 56–65. https://doi.org/10.1016/j.jmat.2018.12.003.

Bustillo-Lecompte, C. F., Kakar, D., & Mehrvar, M. (2018). Photochemical treatment of

benzene, toluene, ethylbenzene, and xylenes (BTEX) in aqueous solutions using advanced oxidation processes: Towards a cleaner production in the petroleum refining and petrochemical industries. *Journal of Cleaner Production*, *186*, 609–617. https://doi.org/10.1016/j.jclepro.2018.03.135.

Costa, G. S., Costa, M. J. S., Oliveira, H. G., Lima, L. C. B., Luz, G. E., Cavalcante, L. S., & Santos, R. S. (2020). Effect of the applied potential condition on the photocatalytic properties of $Fe_2O_3|WO_3$ heterojunction films. *Journal of Inorganic and Organometallic Polymers and Materials*, *30*(8), 2851–2862. https://doi.org/10.1007/s10904-019-01429-0.

Elci, A., Demirtas, O., Ozturk, I. M., Bek, A., & Nalbant Esenturk, E. (2018). Synthesis of tin oxide-coated gold nanostars and evaluation of their surface-enhanced Raman scattering activities. *Journal of Materials Science*, *53*(24), 16345–16356. https://doi.org/10.1007/s10853-018-2792-4.

Ferrari-Lima, A. M., De Souza, R. P., Mendes, S. S., Marques, R. G., Gimenes, M. L., & Fernandes-Machado, N. R. C. (2015). Photodegradation of benzene, toluene and xylenes under visible lightapplying N-doped mixed TiO_2 and ZnO catalysts. *Catalysis Today*, *241*(PA), 40–46. https://doi.org/10.1016/j.cattod.2014.03.042.

Fischer, K., Gawel, A., Rosen, D., Krause, M., Abdul Latif, A., Griebel, J., Prager, A., & Schulze, A. (2017). Low-Temperature Synthesis of Anatase/Rutile/Brookite TiO_2 Nanoparticles on a Polymer Membrane for Photocatalysis. *Catalysts*, *7*(7), 209. https://doi.org/10.3390/catal7070209.

Fouad, D. E., Zhang, C., El-Didamony, H., Yingnan, L., Mekuria, T. D., & Shah, A. H. (2019). Improved size, morphology and crystallinity of hematite (α-Fe_2O_3) nanoparticles synthesized via the precipitation route using ferric sulfate precursor. *Results in Physics*, *12*(January), 1253–1261. https://doi.org/10.1016/j.rinp.2019.01.005.

Hir, Z. A. M., Abdullah, A. H., Zainal, Z., & Lim, H. N. (2017). Photoactive Hybrid Film Photocatalyst of Polyethersulfone-ZnO for the Degradation of Methyl Orange Dye: Kinetic Study and Operational Parameters. *Catalysts*, *7*(11), 1–16. https://doi.org/10.3390/catal7110313.

Hir, Z. A. M., Moradihamedani, P., Abdullah, A. H., & Mohamed, M. A. (2017). Immobilization of TiO2 into polyethersulfone matrix as hybrid film photocatalyst for effective degradation of methyl orange dye. *Materials Science in Semiconductor Processing*, *57*(2017), 157–165. https://doi.org/10.1016/j.mssp.2016.10.009.

Karmaoui, M., Jorge, A. B., McMillan, P. F., Aliev, A. E., Pullar, R. C., Labrincha, J. A., & Tobaldi, D. M. (2018). One-Step Synthesis, Structure, and Band Gap Properties of SnO2 Nanoparticles Made by a Low Temperature Nonaqueous Sol-Gel Technique. *ACS Omega*, *3*(10), 13227–13238. https://doi.org/10.1021/acsomega.8b02122.

Leusch, F., & Bartkow, M. (2010). A short primer on benzene, toluene, ethylbenzene and xylenes (BTEX) in the environment and in hydraulic fracturing fluids. *Griffith University - Smart Water Center*, *October 2020*, 1–8. https://www.ehp.qld.gov.au/management/coal-seam-gas/pdf/btex-report.pdf.

Parthibavarman, M., Karthik, M., & Prabhakaran, S. (2018). Facile and one step synthesis of WO_3 nanorods and nanosheets as an efficient photocatalyst and humidity sensing material. *Vacuum*, *155*(May), 224–232. https://doi.org/10.1016/j.vacuum.2018.06.021.

Singh, M., Goyal, M., & Devlal, K. (2018). Size and shape effects on the band gap of semiconductor compound nanomaterials. *Journal of Taibah University for Science*, *12*(4), 470–475. https://doi.org/10.1080/16583655.2018.1473946.

Syazwani, O. N., Mohd Hir, Z. A., Mukhair, H., Mastuli, M. S., & Abdullah, A. H. (2018). Designing visible-light-driven photocatalyst of Ag_3PO_4/CeO_2 for enhanced photocatalytic activity under low light irradiation. *Journal of Materials Science: Materials in Electronics*, *30*(1), 415–423. https://doi.org/10.1007/s10854-018-0306-4.

WHO. (2004). *Guidelines for Drinking-Water Quality* (2nd Ed.).